Growth mechanism of atomic-layer-deposited TiAlC metal gate based on $TiCl_4$ and TMA precursors*

Jinjuan Xiang(项金娟)[1], Yuqiang Ding(丁玉强)[2], Liyong Du(杜立永)[2], Junfeng Li(李俊峰)[1], Wenwu Wang(王文武)[1], and Chao Zhao(赵超)[1,†]

[1] *Key Laboratory of Microelectronics Devices & Integrated Technology, Institute of Microelectronics, Chinese Academy of Sciences, Beijing* 100029, *China*

[2] *Chemical and Material Engineering, Jiangnan University, Wuxi* 214122, *China*

(Received 4 November 2015; revised manuscript received 14 November 2015; published online 25 January 2016)

TiAlC metal gate for the metal-oxide-semiconductor field-effect-transistor (MOSFET) is grown by the atomic layer deposition method using $TiCl_4$ and $Al(CH_3)_3$(TMA) as precursors. It is found that the major product of the $TiCl_4$ and TMA reaction is TiAlC, and the components of C and Al are found to increase with higher growth temperature. The reaction mechanism is investigated by using x-ray photoemission spectroscopy (XPS), Fourier transform infrared spectroscopy (FTIR), and scanning electron microscope (SEM). The reaction mechanism is as follows. Ti is generated through the reduction of $TiCl_4$ by TMA. The reductive behavior of TMA involves the formation of ethane. The Ti from the reduction of $TiCl_4$ by TMA reacts with ethane easily forming heterogenetic $TiCH_2$, $TiCH{=}CH_2$ and TiC fragments. In addition, TMA thermally decomposes, driving Al into the TiC film and leading to TiAlC formation. With the growth temperature increasing, TMA decomposes more severely, resulting in more C and Al in the TiAlC film. Thus, the film composition can be controlled by the growth temperature to a certain extent.

Keywords: atomic layer deposition, metal gate, TiAlC, reaction mechanism

PACS: 73.40.Qv **DOI:** 10.1088/1674-1056/25/3/037308

1. Introduction

The integrated circuit (IC) technology is the key in the modern information industry. In order to obtain high performance and low power, the feature size of the IC technology continually shrinks. For the 45 nm technology node, high dielectric material (high-*k*) and metal gate are introduced into the conventional metal–oxide–semiconductor (MOS) field-effect-transistor (FET).[1] For the 22 nm technology node, FinFET or Tri-gate structure is employed to continue equivalently scaling the MOSFET.[2,3] One of the main challenges for the introduction of high-*k* and metal gate is the appropriate work function of metal gate.[4–6] Titanium–aluminum-(Ti/Al) based metal has received much attention as N-type work function metal in the past few years. For example, TiAlN metal is highly considered as N-type metal gates in 45 nm and 32 nm product by Intel, due to its proper work function.[1,7] The Ti/Al-based metal has been widely deposited by physical vapor deposition (PVD) technique.[8,9] Although PVD has various advantages, its inherent nature does not allow conformal film growth, which is required for three-dimensional FinFET devices of 22 nm technology node and beyond. Atomic layer deposition (ALD) is a method based on sequential self-saturated surface reactions, leading to the controlled layer-by-layer growth of thin films at molecular level. The unique, generally self-limiting, growth mechanism of the ALD process gives better thickness control, thickness uniformity and conformality, than other deposition techniques.[10,11] Therefore ALD technology can offer the best solution to the problems accompanied by the scaling of MOSFET shrinking devices. However, ALD Ti/Al-based N-type work function metal is rather difficult to grow due to the precursor limit. There are only few publications about the N-type metal gate prepared by ALD until now. Ragnarsson *et al.* used a new ALD TiAl process to demonstrate conformal low threshold voltage bulk FinFET devices.[12] Jeon *et al.* and Kim *et al.* got ALD TiC–TiN film and ALD TiC film with acceptable effective work function (EWF).[13,14] In particular, the reaction mechanism of ALD N metal process is rarely reported.

In our previous work, we have grown the TiAlC film as N-type work function metal by thermal ALD.[15] The grown TiAlC film has an effective work function of 4.49 eV which is suitable for FinFET application. In this study, we investigated the reaction mechanism of the ALD TiAlC film grown by $TiCl_4$ and $Al(CH_3)_3$ (TMA) reaction, based on the x-ray photoemission spectroscopy (XPS), Fourier transform infrared spectroscopy (FTIR), and scanning electron microscope (SEM) measurements.

2. Experiment

TiAlC was grown using $TiCl_4$ as Ti precursor and TMA as Al precursor by thermal ALD on Beneq ALD tool TFS200.

*Project supported by the Key Technology Study for 16/14 nm Program of the Ministry of Science and Technology of China (Grant No. 2013ZX02303).

†Corresponding author. E-mail: zhaochao@ime.ac.cn

© 2016 Chinese Physical Society and IOP Publishing Ltd

Both of the $TiCl_4$ and TMA were vaporized from liquid source containers kept at 21 °C and introduced into ALD reactor chamber by N_2 carrier gas. The reaction pressure was about 1.5 millibar. One deposition cycle consists of $TiCl_4$ pulse, N_2 purge, TMA pulse, and N_2 purge. The deposition temperature was changed in the range of 200 °C to 400 °C in the cold wall reactor. The gas flow was cross flow. The composition and bonding properties were measured by XPS and FTIR. The surface topography was evaluated by SEM.

3. Results and discussion

Figure 1 shows the composition of the films deposited at 200 °C, 300 °C, and 400 °C as a function of XPS etching time. The C 1s signal before etching is larger than that after ∼ 120 s etching, and this is due to the adventitious contamination. The C 1s signal is nearly unchanged after ∼ 120 s etching, and this indicates that the Ar^+ etching of ∼ 120 s is effective to eliminate the adventitious contamination and the natural oxidation layer on the film surface. Table 1 gives the component content of each element from the XPS results in Fig. 1. It can be seen that the major components of the film grown at 200 °C are Ti and O. The Ti content is 61% and the O content is 36%. There are also 2% C and 1% Al. As for the film grown at 300 °C, the Ti, C, O, and Al components are 36%, 40%, 20%, and 4%. For the film grown at 400 °C, the Ti, C, O, and Al components are 34%, 51%, 7%, and 8%.

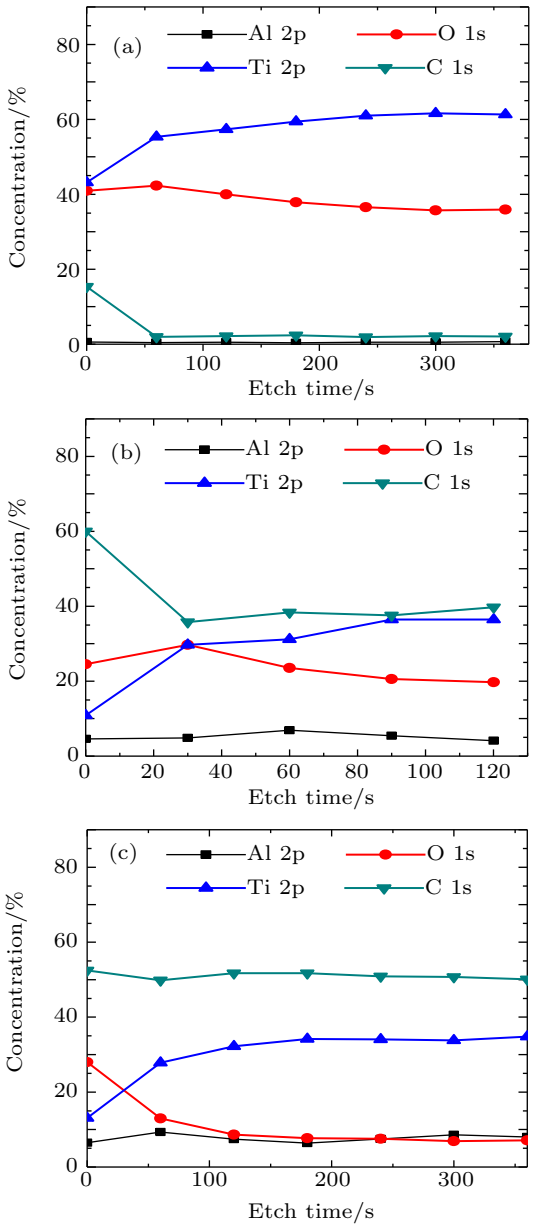


Fig. 1. (color online) The composition of the as-deposited films grown at (a) 200 °C, (b) 300 °C, and (c) 400 °C measured by XPS.

Table 1. The composition of the as-deposited films grown at different temperatures measured by XPS.

	Ti	C	Al	O
200 °C	61	2	1	36
300 °C	36	40	4	20
400 °C	34	51	8	7

Figure 2 gives the XPS spectra of the C 1s, Ti 2p, Al 2p, and O 1s of the films grown at different temperatures. The signals are collected after 120 s etching and all the element contents tend to be stable. For the C 1s spectrum in Fig. 2(a), the C 1s peaks at 281.8 eV, 282.7 eV, and 284.8 eV are from C–Ti, C–Al, and C–H bonds, respectively. It can be seen that only weak C–Ti signal appears at 200 °C. While for film growth at 300 °C and 400 °C, both C–Ti and C–Al signals are detected. For the Ti 2p spectrum in Fig. 2(b), the binding energies of ∼ 454.9 eV for the Ti $2p_{3/2}$ and ∼ 460.9 eV for Ti $2p_{1/2}$ are typical to the Ti–C bond, and the binding energies of ∼ 457 eV for the Ti $2p_{3/2}$ and ∼ 463 eV for Ti $2p_{1/2}$ are typical to the Ti–O bond. It can be seen that both Ti–C and Ti–O bonds appear for the three films. However, the Ti–O signal decreases significantly when the growth temperature increases. The Ti–O signal is rather weak at 400 °C. These results are consistent with the remarkable decrease of O content when the growth temperature increases, as shown in Fig. 1 and Table 1. For the Al 2p spectrum in Fig. 2(c), the peaks at ∼ 73.6 eV and ∼ 74.7 eV are attributed to Al–C and Al–O bonds, respectively. It can be seen that only Al–O bonds are found for the film at 200 °C. Both Al–O and Al–C bonds appear for the film at 300 °C. For the film grown at 400 °C, the Al–C bond is dominant. For the O 1s spectrum in Fig. 2(d), the peak at ∼ 531 eV is from Ti–O, and the peak at ∼ 532 eV is from Al–O. It can be seen that the dominant component is Ti–O for the three films. Consequently, the above XPS results are consistent.

The oxygen component in the grown film is from the exposed atmosphere after film growth but not from the ALD process. This is because there is no oxygen supply in the ALD precursors ($TiCl_4$ and TMA here) or in the ALD reaction chamber, so no oxygen should appear in the grown film. However, when the grown film is exposed to the atmosphere,

the film can be oxidized by the O_2 in the atmosphere. As a result, the oxygen component should be excluded from each grown film. In other words, the film grown at 200 °C is Ti with nearly negligible C. The film grown at 300 °C and 400 °C is TiAlC. The oxidation of TiAlC film can be avoided in the real fabrication of MOS devices. In the device fabrication process, after the growth of TiAlC film, ALD TiN is *in situ* deposited in the same ALD chamber. Then the TiN/TiAlC sample is transferred from ALD chamber to another ALD chamber (for ALD W) within 2 min for metal W deposition. The metal W can protect the TiN/TiAlC films from being oxidized, so the oxidation of ALD TiAlC is rather negligible.

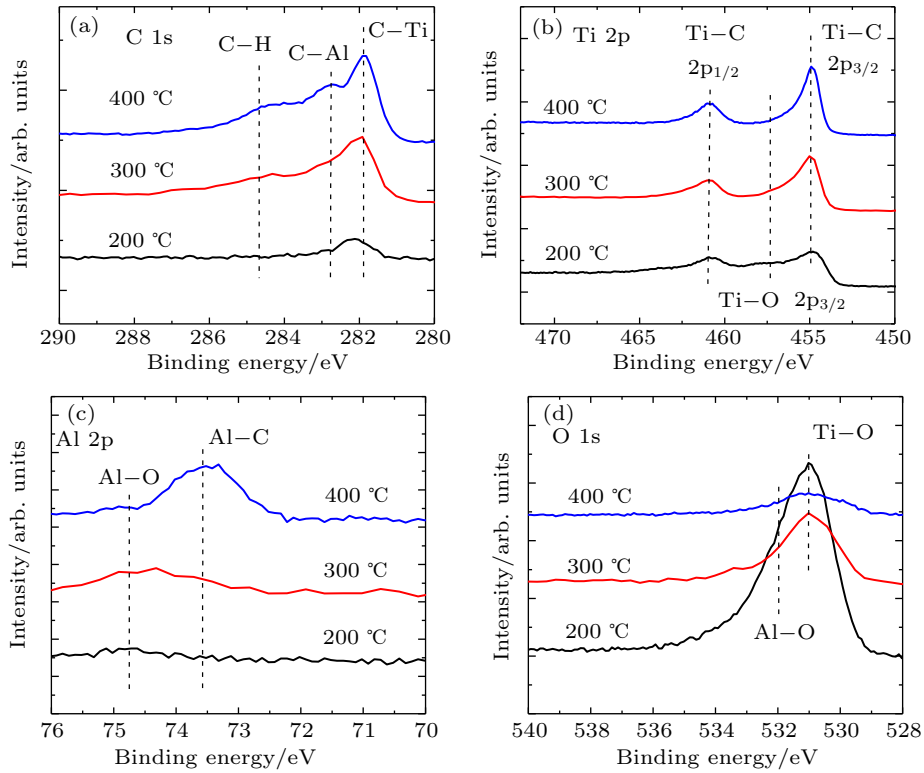


Fig. 2. (color online) XPS spectra of (a) C 1s, (b) O 1s, (c) Ti 2p, and (d) Al 2p of the as-deposited films grown at different temperatures.

Figure 3 gives the cross section and surface morphology of the deposited films grown at 200 °C, 300 °C, and 400 °C. It can be seen that the film grown at 200 °C peels off from the Si substrate when exposed to the atmosphere, while the films grown at 300 °C and 400 °C have improved smooth surfaces. Figure 4 gives the AFM (atomic force microscopy) pictures. The RMS (root mean square) are estimated to be 18.3 nm, 0.358 nm, and 0.258 nm for the films deposited at 200 °C, 300 °C, and 400 °C, respectively. These data are consistent with the SEM results. This can be explained as follows: The film grown at lower temperature is relatively loose and more prone to be oxidized by the O_2 or H_2O in the atmosphere, which may lead to the peeling phenomenon. The film grown at higher temperature is very dense and has strong resistance to the O_2 and H_2O in the air. Thereby, it has lower O concentration. This is coincident with the XPS results.

In order to further investigate the growth mechanism, the FTIR spectra were measured. Figure 5 shows the FTIR spectra of the as-deposited film at the three different temperatures. The peaks at 2918 cm^{-1} and 2850 cm^{-1} indicate the existence of $–CH_2$, while the peak located around 860 cm^{-1} stands for the existence of $–CH{=}CH_2$. All the $–CH_2$ and $–CH{=}CH_2$ signals are enhanced along with the increase of the growth temperature.

According to the results described above, we make the following reasonable speculation about the growth mechanism. The reductive behavior of $Al(CH_3)_3$ involves the formation of ethane, which has been found by other researchers on ALD manufacturing Cu film.[16] The XPS results suggest that the pure titanium metal was generated through the reduction of $TiCl_4$ by TMA. Then Ti reacts with ethane forming heterogenetic $TiCH_2$, $TiCH{=}CH_2$, and TiC fragments.[17] Meanwhile, TMA thermally decomposes, driving Al doping into the film and leading to TiAlC formation. The higher the temperature is, the easier the reaction happens. The above conclusion is further confirmed by FTIR, where the signals of $–CH{=}CH_2$ (around 860 cm^{-1}) and $–CH_2$ (approximately 2918 cm^{-1}, 2850 cm^{-1}) exist in all samples, and the signals are enhanced obviously as the temperature increases.

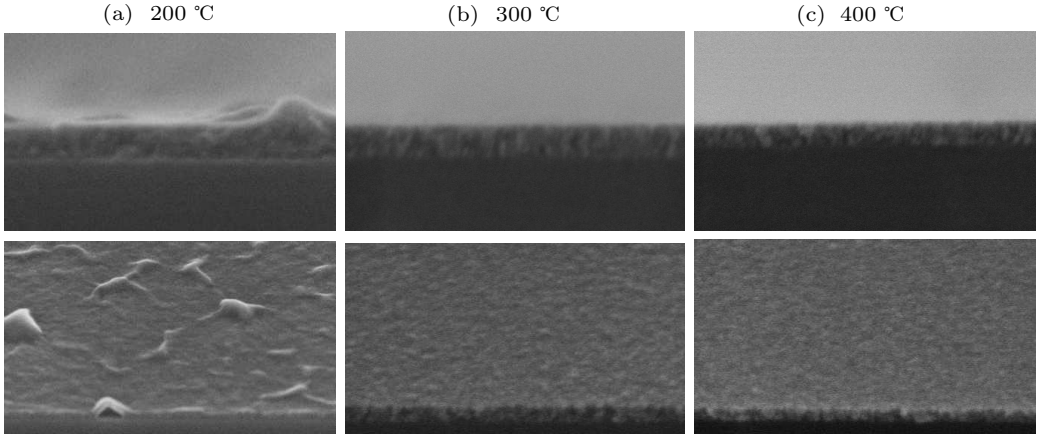


Fig. 3. The cross section (top) and surface morphology (bottom) of the as-deposited film grown at (a) 200 °C, (b) 300 °C, and (c) 400 °C.

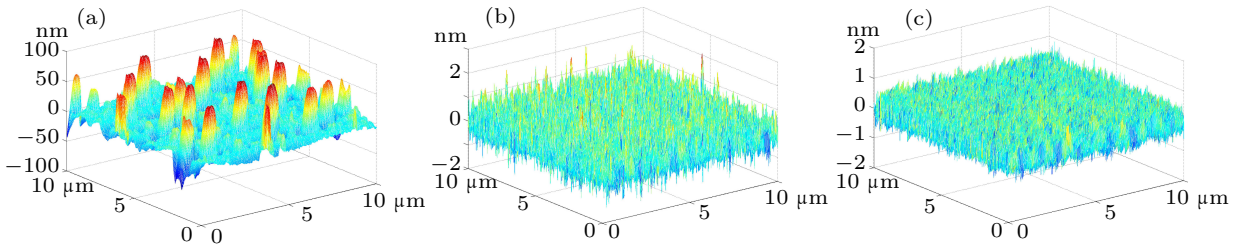


Fig. 4. (color online) The surface roughness pictures of the as-deposited films grown at (a) 200 °C, (b) 300 °C, and (c) 400 °C.

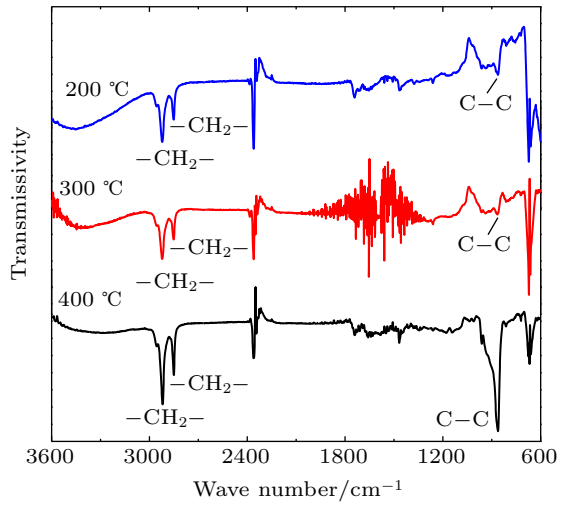


Fig. 5. (color online) The FTIR spectra of the as-deposited films grown at 200 °C, 300 °C, and 400 °C.

4. Conclusion

TiAlC metal gate was grown by using $TiCl_4$ and TMA as precursors. Ti is generated through the reduction of $TiCl_4$ by TMA. The reductive behavior of TMA involves the formation of ethane. The Ti from the reduction of $TiCl_4$ by TMA reacts with ethane forming heterogenetic $TiCH_2$, $TiCH{=}CH_2$, and TiC fragments. In addition, TMA thermally decomposes, driving Al into the TiC film and leading to TiAlC formation. With the growth temperature increasing, TMA decomposes more severely, leading to more C and Al in the TiAlC film. Thus, the film composition can be controlled by the growth temperature to a certain extent.

References

[1] Mistry K, Allen C, Auth C, *et al.* 2007 *IEDM Technical Digest. IEEE International*, December 10–12, 2007, Washington, USA, pp. 247–250
[2] King K J 2012 *Symposium on VLSI Technology* (Short course)
[3] Jan C H, Bhattacharya U, Brain R, *et al.* 2012 *IEDM Technical Digest. IEEE International*, December 10–13, 2012, Sanfransico, USA, 3.1.1–3.1.4
[4] Yang Z C, Huang A P and Xiao Z S 2010 *Physics* **39** 113 (in Chinese)
[5] Han K, Wang X L, Yang H and Wang W W 2013 *Chin. Phys. B* 22 117701
[6] Huang A P, Zheng X H, Xiao Z S, Yang Z C, Wang M, Paul K C and Yang X D 2011 *Chin. Phys. B* **20** 097303
[7] Packan P, Akbar S, Armstrong M, Bergstrom D, Brazier M, Deshpande H, Dev K, Ding G, Ghani T and Golonzka O 2009 *IEDM Technical Digest. IEEE International*, 2009, Washington, USA, pp. 1–4
[8] Han K, Ma X, Yang H and Wang W 2013 *J. Semicond.* **34** 076003
[9] Cui H, Luo J, Xu J, Gao J, Xiang J, Tang Z, Wang X, Lu Y, He X, Li T, Tang B, Yu J, Yang T, Yan J, Li J, Zhao C and Ye T 2015 *Vacuum* **119** 185
[10] George S M 2010 *Chem. Rev.* **110** 111
[11] Puurunen R L 2005 *J. Appl. Phys.* **97** 121301
[12] Ragnarsson L A, Chew S A, Dekkers H, *et al.* 2014 *Symposium on VLSI Technology, Digest of Technical Papers*, Juan 9–12, 2014, Hawaii, USA, pp. 1–2
[13] Jeon S and Park S 2010 *J. Electrochem. Soc.* **157** H930
[14] Kim C K, Ahn H J, Moon J M, Lee S, Moon D, Park J S, Cho B J, Choi Y K and Lee S H 2015 *Solid-State Electron.* **114** 90
[15] Xiang J, Li T, Zhang Y, Wang X, Gao J, Cui H, Yin H, Li J, Wang W, Ding Y, Xu C and Zhao C 2015 *ECS J. Solid State Sci. Technol.* **4** 441
[16] Vidjayacoumar B, Emslie D J H, Blackwell J M, Clendenning S B and Britten J F 2010 *Chem. Mater.* **22** 4854
[17] Honma K 1995 *J. Chin. Chem. Soc.* **42** 371